Volume 19, Number 1, 2026. pp. 31-40

Jordan Journal of Physics

ARTICLE

Influence of Gallium Doping on the Electrical Performance of P3HT Thin-film Transistors Enriched by ZnO Nanoparticles

M. Ba[a], M. Erouel[a], M. Jdir[a], S. Mansouri[b], S. Mrabet[a], A. Bouloufa[c], Z. Ben Ayadi[a], C. Vázquez-Vázquez[d] and L. El Mir[a]

[a] *Laboratory of Physics of Materials and Nanomaterials applied at Environment (LaPhyMNE) LR05ES14, Faculty of Sciences of Gabes, Gabes University, Erriadh City, Zrig, 6072 Gabes, Tunisia.*

[b] *Faculty of Sciences and Technology in Sidi Bouzid, 9100, Agricultural University Campus 9100 - BP - No. 380, Kairouan University, Tunisia.*

[c] *Laboratory of Electrochemistry and Materials, University Ferhat Abbas Sétif-1, Algeria.*

[d] *Laboratory of Magnetism and Nanotechnology (NANOMAG), Department of Physical Chemistry, Faculty of Chemistry, Universidade de Santiago de Compostela, 15782 Santiago de Compostela, Spain.*

DOI: **https://doi.org/10.47011/19.1.4**

Received on: 05/11/2024; *Accepted on: 20/01/2025*

Abstract: In the present work, p-type organic field-effect transistors based on poly (3-hexylthiophene) (P3HT) enriched by gallium doped-zinc oxide (GZO) nanoparticle thin films as the active layer were fabricated using the sol-gel technique coupled with spin-coating method and characterized using various techniques. The morphology of the thin films was analyzed using atomic force microscopy (AFM) and scanning electron microscopy (SEM) techniques, and their optical properties were investigated using the UV-Vis-IR spectroscopy technique. In order to investigate the effect of Ga doping concentration on the electrical performances of the organic thin-film transistors (OTFTs) based on P3HT:GZO thin films, the current-voltage (*I-V*) measurements were carried out in the dark and in daylight using a Keithley 2612B Source Meter. The results demonstrate the ability to control both threshold voltage (V_{th}) and hysteresis by adjusting the Ga doping concentration within the active layer of the transistor devices. Moreover, the fabricated OTFT-P3HT:GZO devices exhibited significantly high performance, achieving a current ratio (I_{on}/I_{off}) of 3.5×10^3 with 1% Ga loading and demonstrating a 100-fold enhancement in field-effect saturation mobility (μ_{sat}) with 3% Ga loading, thereby showcasing their promising potential in a variety of practical applications, including cost-effective photodetectors and sensors.

Keywords: ZnO:Ga nanoparticles, P-type OTFT-P3HT:GZO, Gallium loading effect, Electrical properties, OTFT device performance.

1. Introduction

The highlighting of the semiconducting nature of π-conjugated polymers in their undoped state has paved the way for real development in organic electronics. However, due to the low conductivity inherent in organic semiconductors, this new category of electronics does not aspire to match the electrical performance of traditional electronics with the intention of competing with it in the future. Instead, the goal of organic electronics lies in the development of new cost-effective, portable, flexible, and even disposable applications, not achievable with inorganic electronics. Indeed, the ability of materials used in organic electronic devices to dissolve in solution provides the opportunity for the adoption of more cost-

Corresponding Authors: Mohamadou Ba **Email**: bamohamadou19@gmail.com
Lassaad EL MIR **Email**: Lassaad.ElMir@fsg.rnu.tn

effective manufacturing methods than those used in traditional electronics, such as centrifugal spin coating or printing techniques such as ink-jet or screen printing. Furthermore, the mechanical properties of polymers enable the development of electronics on flexible substrates, paving the way for new portable applications that are unattainable in traditional electronics, such as smart textiles or flexible screens.

Organic electronics primarily relies on three devices that were initially developed in the 1980s: organic photovoltaic cells (OPVs) in 1986, organic field-effect transistors (OFETs) in 1986, and organic light-emitting diodes (OLEDs) in 1987 [1-3]. From an industrial perspective, OLEDs are the devices closest to large-scale commercialization, while transistors are the essential basic components for the development of more complex circuits. Since the production of the first organic transistors, significant progress has been made in both electrical performance and reliability. These advancements have been made possible through the synthesis of new air-stable organic semiconductors with increasingly higher mobility [4, 5]. However, the advancements made in recent years cannot be solely attributed to the improvement of semiconductor characteristics. Indeed, these progressions also result from a deeper understanding of the mechanisms governing charge transport in organic transistors. Nevertheless, many phenomena still need clarification, particularly concerning the interfaces between the organic semiconductor and other constituent materials of the transistor. In reality, the quality of the interface between the contact electrodes and the semiconductor plays a crucial role in charge injection into the transistor channel. Similarly, the quality of the interface between the organic semiconductor and the dielectric is essential for the charge transport in the same channel. Another significant factor that affects the performance of OTFT devices is the relatively low field-effect mobility of charge carriers in the majority of organic semiconductors when compared to the inorganic semiconductors.

In order to improve electrical properties, since charge carrier concentration is strongly influenced by doping concentration, inorganic nanoparticles can be integrated into the organic polymers. Undoped and doped-ZnO nanoparticles find extensive applications as acceptors in hybrid semiconductor layers for electronic devices and as materials for electron extraction [6-8].

In the present work, we investigate the influence of gallium doping concentration (0 to 3%) on the electrical performance of OTFT devices based on P3HT enriched by gallium doped-zinc oxide (GZO) thin-films as the active layer. The objective of this paper is to assess the gallium doping effect on OTFT-P3HT:GZO devices properties, with the aim of improving their electrical performance under ambient conditions. This is achieved by studying the morphological, optical, and electrical properties of the produced devices and to evaluate their suitability for electronic applications. Therefore, the thin films of P3HT pure and P3HT:GZO were fabricated using the sol-gel technique coupled with spin-coating method. This specific technique was chosen due to its numerous advantages, including a large deposition area, straightforward equipment requirements, low fabrication costs, and high precursor homogeneity.

2. Materials and Methods

Through the sol-gel process, we dissolved 16 g of zinc acetate $(CH_3COO)_2$ in 112 mL of methanol, stirring the solution for 15 minutes. Subsequently, 188 mL of ethanol was added to the solution, which was then placed in a 1 L autoclave. Following the method established by L. El Mir and colleagues, ZnO nano-powder aerogels were ultimately generated by evacuating ethanol under supercritical conditions (T_C = 243 °C, P_C = 63.6 bars) [9]. The Poly (3-hexylthiophene) (P3HT) polymer utilized in this investigation was supplied by the Sigma-Aldrich company. The selection of this organic p-type semiconductor for our devices is primarily driven by its notable hole field-effect mobility (10^{-4}-10^{-1}) $cm^2/V{\cdot}s$ attributed to its high regioregularity rate (P3HT-RR); this parameter is crucial to achieve favorable electrical performance in OTFT devices by ensuring thin films with enhanced crystallinity and interchain interactions.

We dispersed 10 mg of nano-powder of P3HT polymer and 100 mg of gallium-doped zinc oxide (GZO) nanoparticles in 1 mL of chlorobenzene solvent, which constitutes the initial step of the process. In order to study the influence of Ga doping on the properties of

P3HT:GZO based OTFT, the Ga doping concentrations were systematically varied from 0 to 3%. Subsequently, the solutions were left under stirring at 80 °C for 2 days to obtain high homogeneity and dispersion. The deposition of the thin films was carried out on both silicon dioxide substrate to fabricate the OTFT devices and glass substrates to study morphological and optical properties. These films were used as the active layer of OTFTs, at room temperature using spin-coating method, employing a speed of 5000 rpm for 10 seconds. Following the deposition, the fabricated devices underwent preheating at 100 °C for 20 minutes on a hot plate to facilitate solvent evaporation and eliminate organic residues.

The fabricated OTFT-P3HT:GZO devices feature a bottom gate/bottom-contact (BG-BC) configuration with a channel length value of L = 20 µm and a width of W = 10 mm, using the silicon dioxide substrate composed of prefabricated chips provided by Fraunhofer IPMS. The gate electrode is formed by heavily doped silicon (n^+-Si) with a dopant concentration of approximately 3 ×.10^{17} cm^{-3}. The insulator film is a silicon dioxide (SiO_2) layer, grown through thermal oxidation with a thickness of (230 ± 10) nm and a capacitance per unit area of C_i = 15 $nF.cm^{-2}$, and no specific surface treatment was applied to the insulator film. The source drain contacts, formed by a 10 nm-thick indium tin oxide (ITO) layer as an adhesion film and a 30 nm-thick gold (Au) layer as the conductive film, are interdigitated to create the conductive channel. The experimental setup adopted for this study is illustrated in Fig. 1.

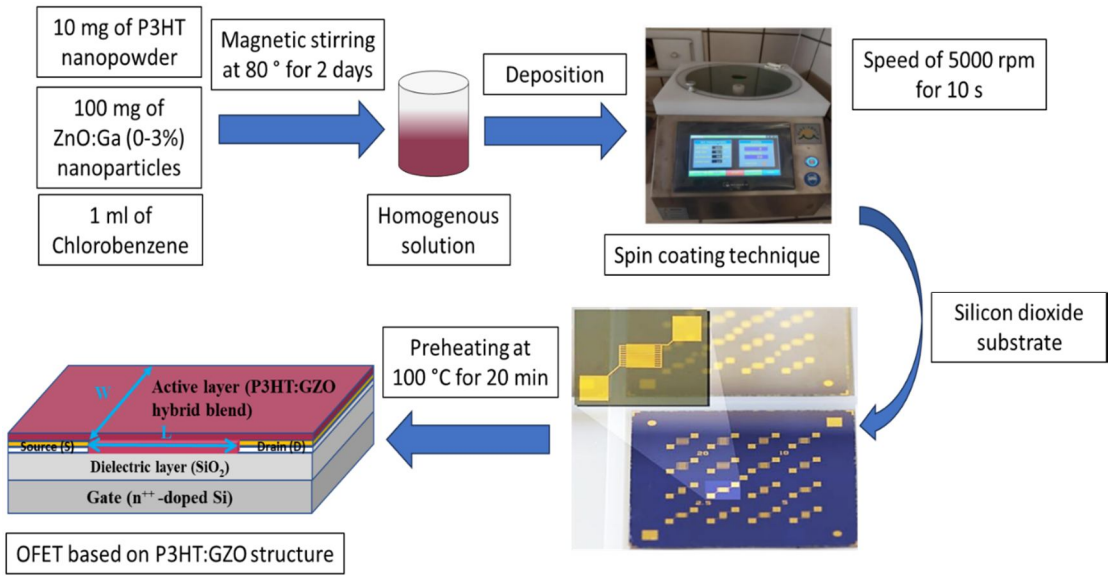

FIG. 1. Experimental procedure.

The electrical measurements were performed in dark and ambient conditions using a Keithley 2612 SourceMeter analyzer. Furthermore, the thin films of P3HT pure and P3HT:GZO were deposited on the glass substrate in order to investigate the morphological and optical properties using atomic force microscopy (AFM), scanning electron microscope (SEM) and UV-Vis-IR spectroscopy (at wavelength range from 200 to 3100 nm) techniques.

3. Results and Discussion

3.1. Morphological Characterization

In order to investigate the morphological structure of the devices' active layer, atomic force microscopy (AFM) and scanning electron microscopy (SEM) techniques were used.

Figure 2 exhibits the topographic images obtained through 2D and 3D atomic force microscopy (AFM) of thin films composed of P3HT pure and P3HT:GZO that were deposited on a glass substrate. The figure depicts a uniformly rough surface of the P3HT pure film (see Fig. 2(a)), and a uniform surface morphology characterized by hexagonal-shaped GZO crystallites distributed within the P3HT polymer matrix in P3HT:GZO thin films (see Fig. 2(b)). Additionally, Fig. 2(b) reveals the presence of fine and rough nanostructures, along with well-organized thin films, suggesting improved electrical performance.

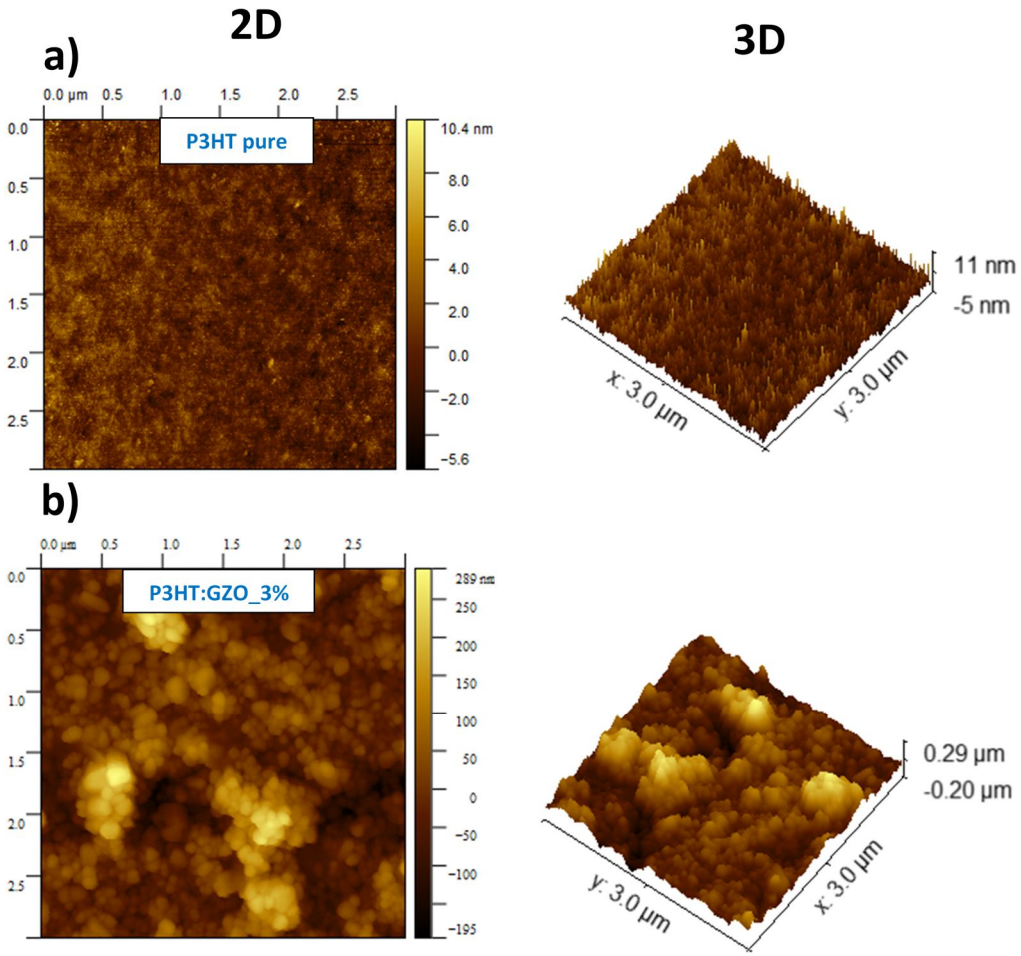

FIG. 2. AFM topographic images of P3HT pure (a), and P3HT:GZO_3% (b) thin films in 2D (left) and 3D (right).

Figure 3 illustrates the SEM images of P3HT pure and P3HT:GZO thin films. Fig. 3(b) presents a homogeneous surface morphology composed of hexagonal crystallites with an average size of about 32 nm, and indicates an agglomeration of porous nanostructures with fine and rough grains in hybrid films.

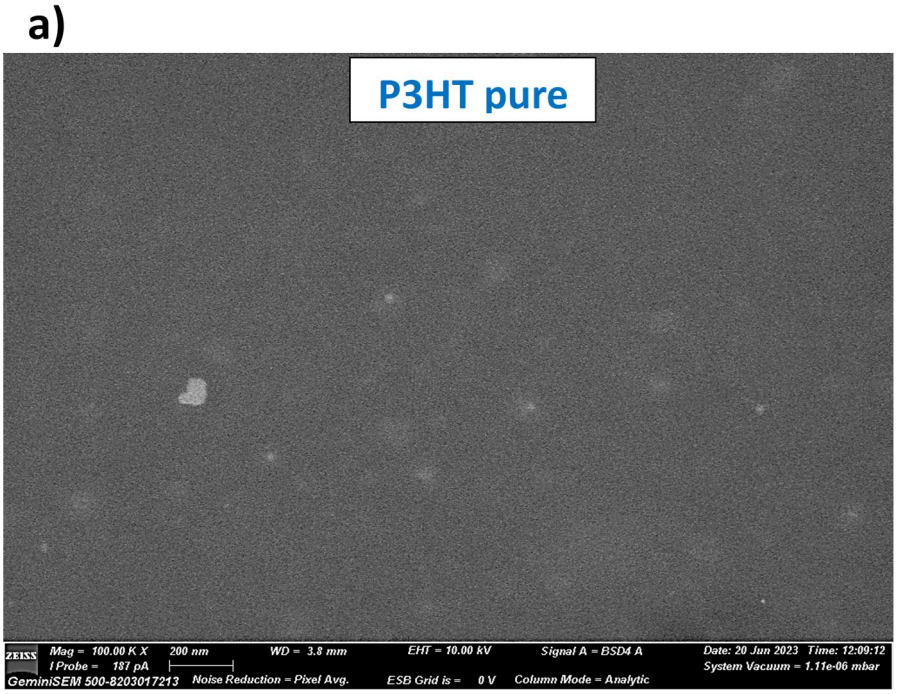

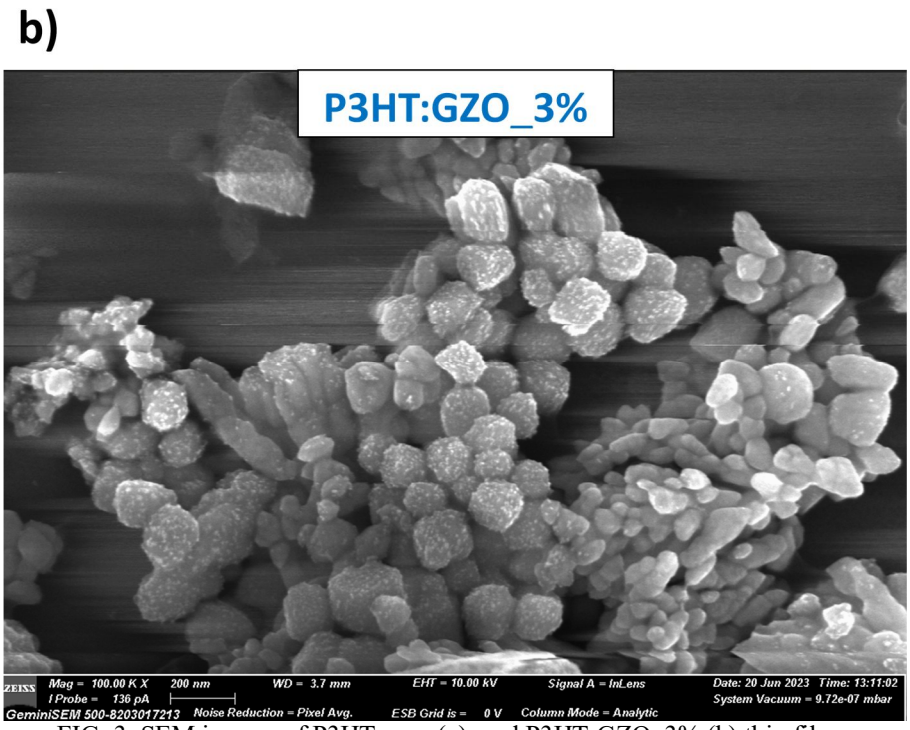

FIG. 3. SEM images of P3HT pure (a), and P3HT:GZO_3% (b) thin films.

3.2. Optical Characterization

To study the optical properties of the active layer of the fabricated devices the UV-Vis-IR spectroscopy technique was utilized. Fig. 4 shows the absorbance spectra of P3HT pure and P3HT:GZO_3% thin films in the wavelength range from 200 to 3100 nm at various gallium doping concentrations (0-3%). The absorbance spectra of hybrid films reveal the appearance of two peaks: a peak located at 370 nm, which corresponds to the ZnO bandgap energy [10], suggesting the existence of GZO nanoparticles within the P3HT polymer. Additionally, another peak at 550 nm, accompanied by a shoulder at around 600 nm in the visible region for the P3HT polymer, attributed to the π-π* transition [11]. On the other hand, the figure illustrates a reduction in peak intensity corresponding to an increase in the Ga doping concentration. This phenomenon can be elucidated by the enhancement in transparency observed in the thin films with the increasing GZO doping concentration, which implies that P3HT:GZO thin films hold potential for utilization in transparent conductive oxide devices.

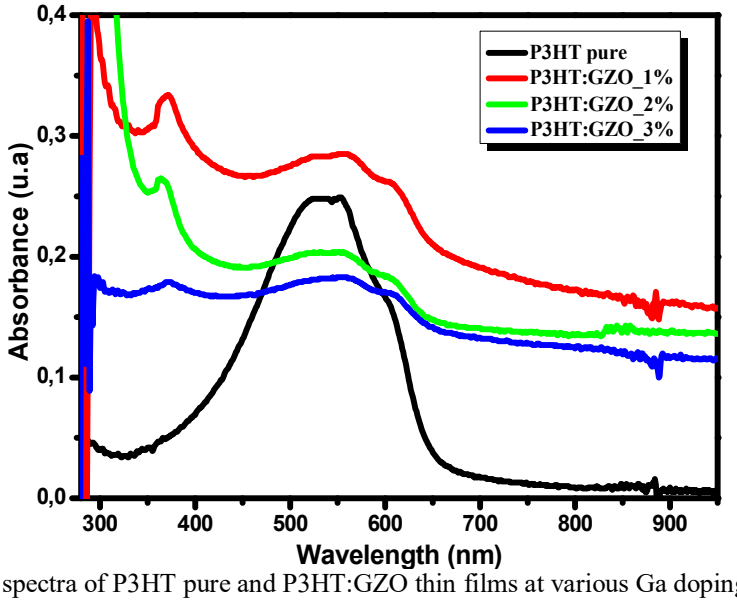

FIG. 4. Absorbance spectra of P3HT pure and P3HT:GZO thin films at various Ga doping concentrations (1-3%).

3.3. Electrical Characterization and Performance

To investigate the effect of Ga doping on the electrical characteristics of organic thin-film transistors utilizing P3HT:GZO at various gallium doping concentrations (0-3%), the current-voltage (*I-V*) measurements were conducted on the devices both in dark and in daylight.

3.3.1 Output Characteristics

The output characteristics corresponding to drain current (I_d) as a function of drain voltage (V_d) with gate voltages V_g varying from 0 to -24 V) of the organic thin-film transistors based on P3HT:GZO at various gallium doping concentration (0-3%), are shown in Fig. 5. As depicted in the figure, the lower drain current (I_d) exhibits excellent linearity with the drain voltage (V_d) in all curves. This observation suggests the establishment of a strong ohmic contact between the metal contacts (Au/ITO) and the semiconductor layer (P3HT:GZO). This is attributed to the formation of Schottky potential barriers for hole injection, arising from the disparity between the work function of gold (Au) and the electronic affinity of P3HT [12]. Additionally, it was observed that the drain current attains saturation (I_{ds}) at elevated drain voltages, indicating the pinch-off of the conductive channel. We also observed that the drain current (I_d) of these devices increases with negative gate voltages (V_g), affirming the P3HT compound as a p-type organic semiconductor, and indicating that the organic transistors operate in the accumulation regime. Furthermore, Fig. 5 illustrates a significant increase in the drain current (I_d) when the Ga doping concentration rises, attaining a tenfold escalation with the transistor OTFT-P3HT:GZO_3% (see Fig. 5(e)). This can be associated with the increase in charge carriers' concentration and, simultaneously, the reduction in density of traps within the conducting channel of the fabricated OTFT devices [13].

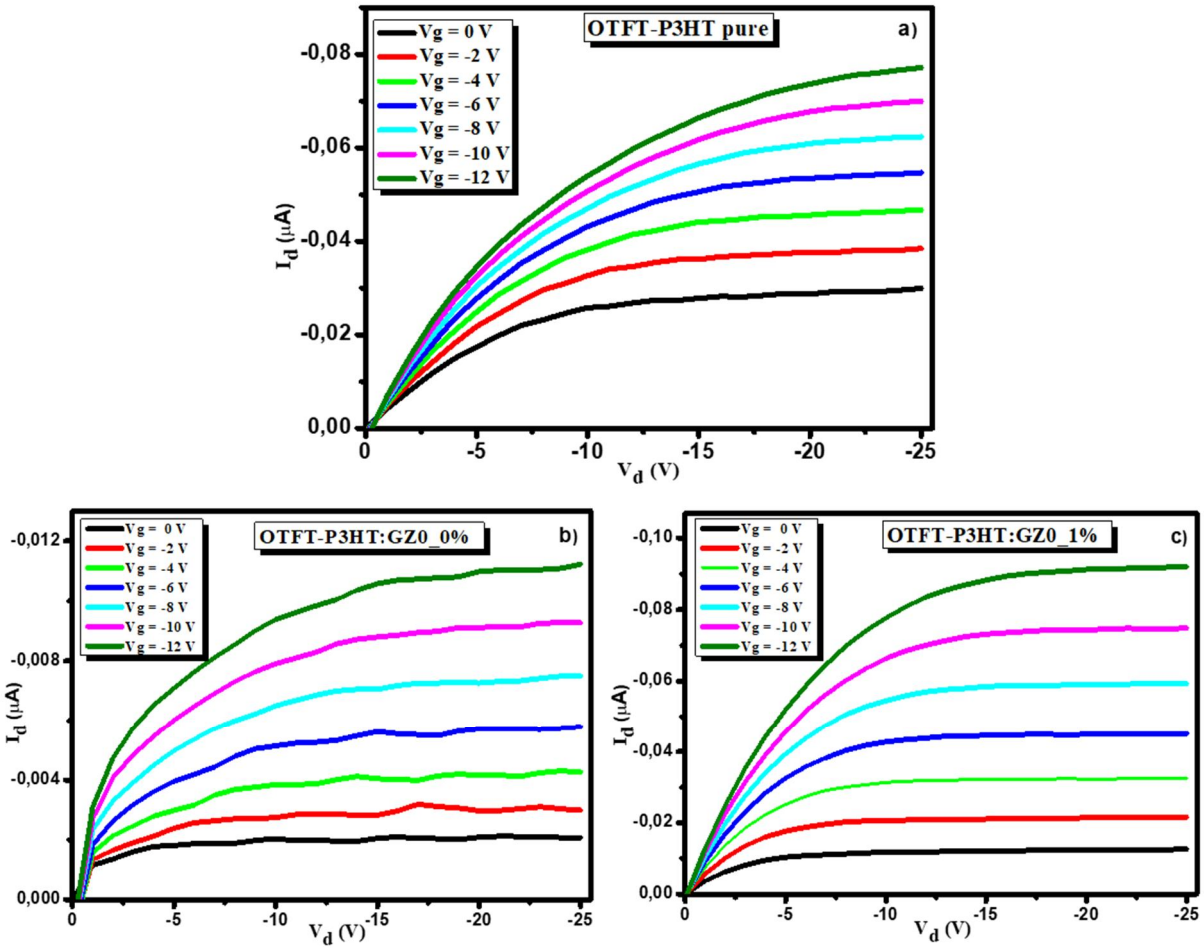

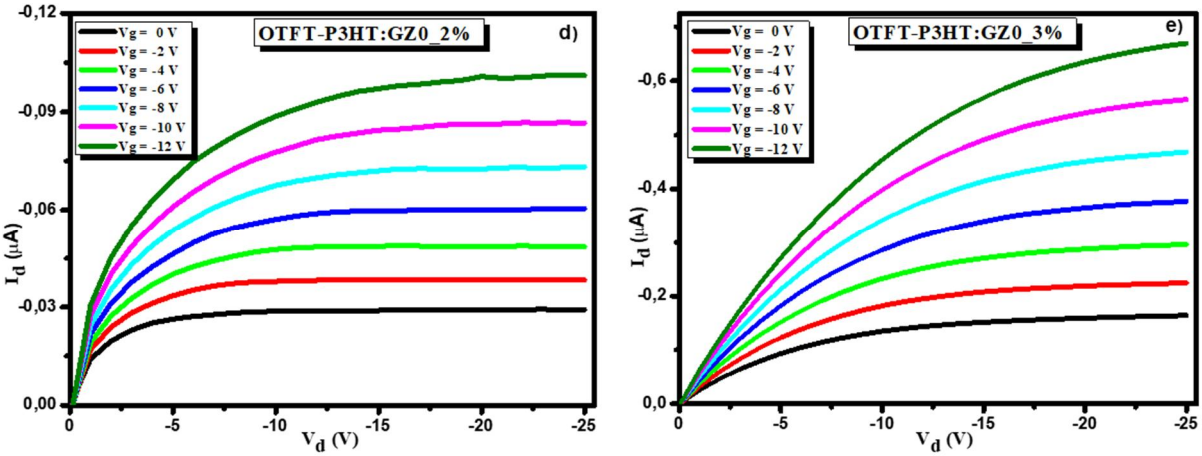

FIG. 5. Output characteristics (drain current (I_d) as a function of drain voltage (V_d) with gate voltages V_g from 0 to -24 V) of OTFTs-P3HT:GZO at various Ga doping concentration (0-3%).

3.3.2 Transfer Characteristics

The transfer characteristics (drain current (I_d) as a function of gate voltage (V_g) with drain voltage (V_d = -20 V) in saturation regime of the fabricated transistors are illustrated in Figs. 6 and 7, and the forward and backward curves of the drain current (I_d) were swept between gate voltages V_g = +10 and -35 V.

The hysteresis phenomenon observed in the transistors' characteristics is often linked to the more or less persistent accumulation of charge carriers in their channel when a voltage variation is applied to their gate. Specifically, for a given gate voltage (V_g), the measured drain current (I_d) varies between the forward sweep (when the transistor switches from the off-state to the on-state) and the backward sweep (when the transistor switches from the on-state to the off-state) of the cycle. This generally reversible phenomenon is commonly observed in most organic transistors, with its nature and intensity depending on the gate dielectric and its interface with the organic semiconductor. Various phenomena occurring at the interface between the semiconductor and dielectric can give rise to clockwise hysteresis. The two most frequently cited factors are charge carrier trapping and, in the context of polymers, bipolaron formation [14, 15].

As shown in Fig. 6, we noticed a considerable decrease in hysteresis for the OTFT-P3HT:GZO_1% and OTFT-P3HT:GZO_3% devices. Actually, a significant variation in the amount of hysteresis (Δh_{hys}) was observed when increasing the Ga doping concentration. Through the analysis of these results, we can confirm that varying the Ga doping concentration in OTFT devices based on P3HT:GZO thin films can effectively control and minimize the amount of hysteresis in the transfer characteristics.

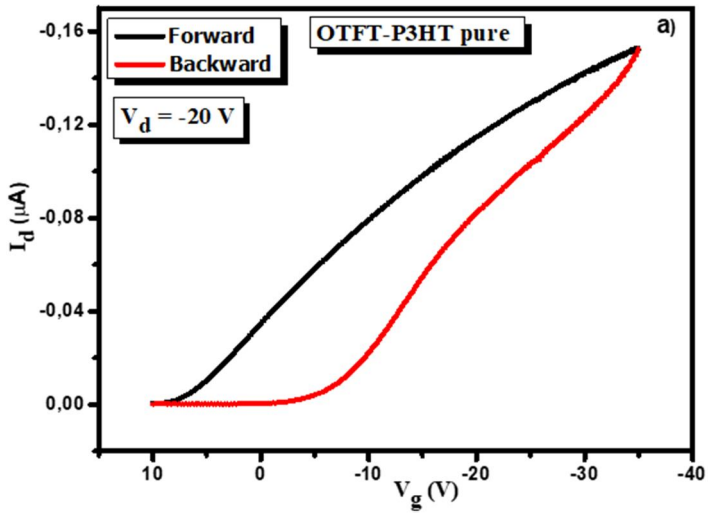

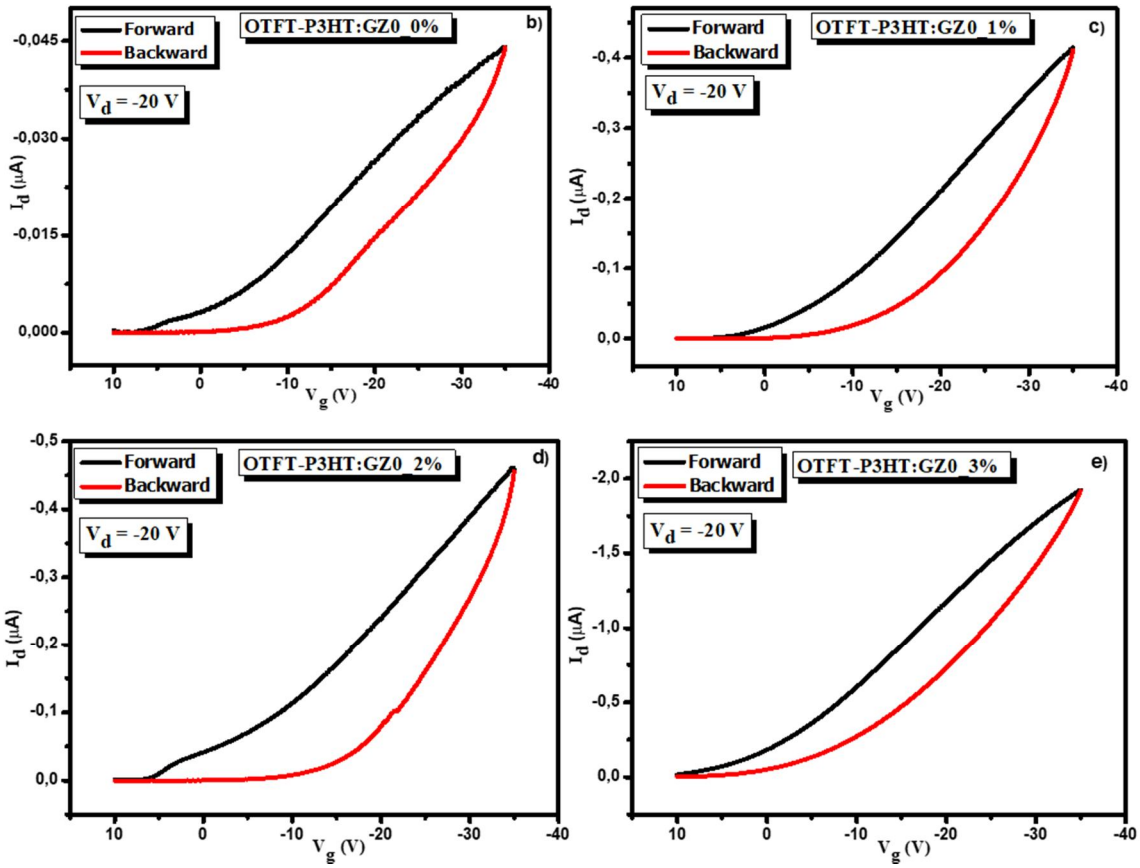

FIG. 6. Hysteresis curves in transfer characteristics (drain current (I_d) as a function of gate voltage (V_g) at drain voltage of V_d = -20 V) in saturation regime of OTFTs-P3HT:GZO at various Ga doping concentration (0-3%).

The examination of the transfer characteristics in the saturated regime, depicted in Fig. 7, enables the extraction of the main transistor parameters including the current ratio (I_{on}/I_{off}), sub-threshold slope (SS), threshold voltage (V_{th}) and saturation field-effect mobility (μ_{sat}) of the transistors as a function of Ga doping concentrations. The parameter extraction is achieved by plotting the square root ($I_d^{1/2}$ versus V_g) on a semi logarithmic scale and the absolute value ($|I_d|$ versus V_g) of the forward drain current in the transfer characteristics (see Fig. 6). Thus, the current ratio and sub-threshold slope are extracted from the absolute value curve, while the threshold voltage (V_{th}) is obtained by the intersection of the slope in saturation regime of the square root curve in the gate voltage axis. The saturation field-effect mobility (μ_{sat}) is given by the following expression:

$$\mu_{sat} = \frac{2L}{WC_i}\left(\frac{\partial\sqrt{I_d}}{\partial V_g}\right)^2 \quad (1)$$

where L represents the channel length, W is width of the conductive channel, C_i is the capacitance per unit area of the insulator layer and $(\frac{\partial\sqrt{I_d}}{\partial V_g})$ corresponds to the slope in saturation regime of the square root curve.

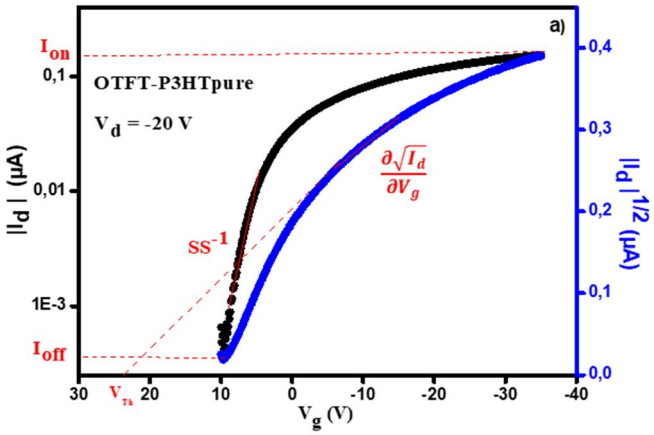

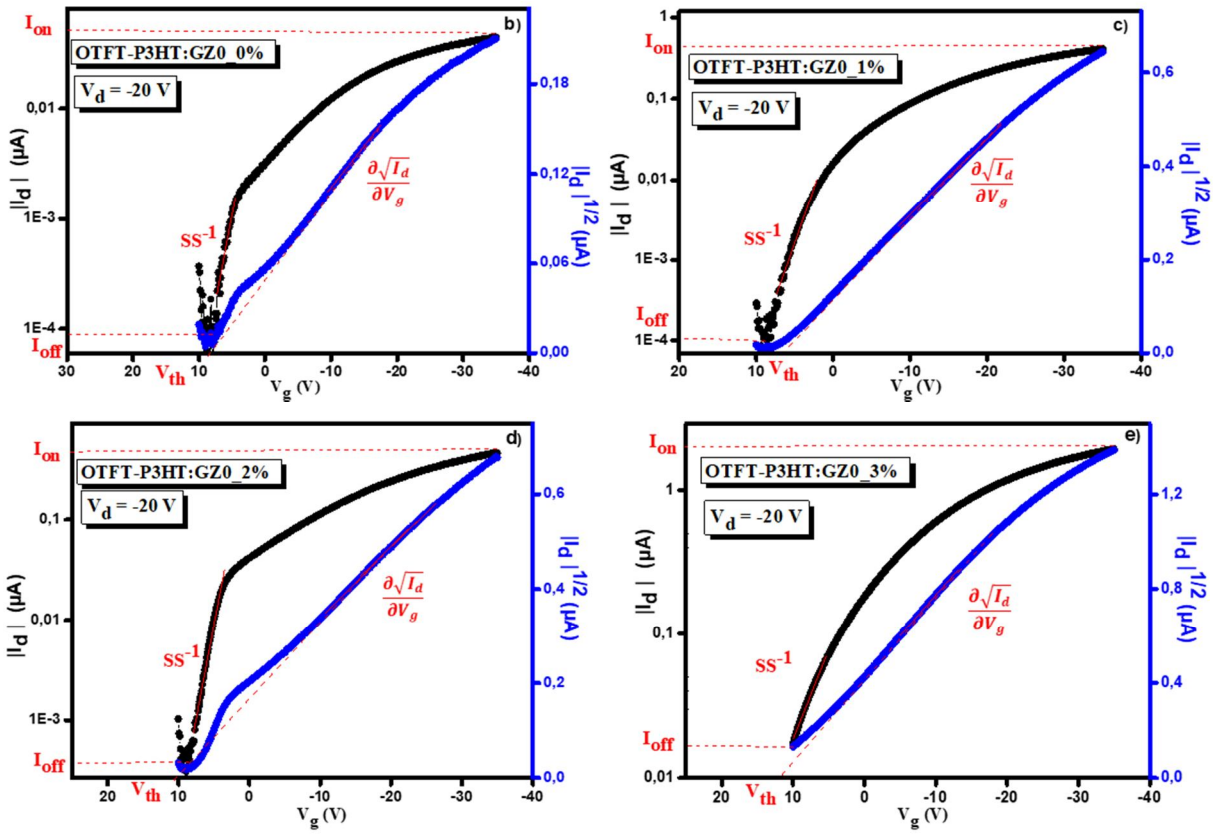

FIG. 7. Plots of ($|I_d|$-V_g) and ($I_d^{1/2}$ -V_g) to extract the key electrical parameters of transistors from the transfer characteristics of OTFTs-P3HT:GZO at various Ga doping concentration (0-3%).

The extracted parameters have been calculated and summarized in Table 1 to highlight the Ga doping concentration effect on the OTFT-P3HT:GZO performances. From the table, it can be noticed that the threshold voltage (V_{th}) values obtained are relatively low (around 10 V) and the sub-threshold voltage (SS) values significantly decrease for the transistors with Ga doping level at 1, 2 and 3%. Basically, the threshold voltage (V_{th}) indicates the gate voltage (V_g) necessary to induce a detectable channel current flow. Meanwhile, the sub-threshold slope (SS) provides insights into the switching speed by assessing the transistor device's turn-on speed. Typically, the low values of these two parameters indicate the efficiency of transistor devices. In general, they are correlated with the presence of trapped charges (N_{trap}) within the semiconductor layer and interface trap density (D_{it}) at the interface between the semiconductor layer and the dielectric insulator [16, 17]. Furthermore, significant enhancements are observed in the table in both the current ratio (I_{on}/I_{off}) and the saturation field-effect mobility of charge carriers (μ_{sat}), crucial factors that dictate the overall performance of transistor devices; which should be as high as possible. The Table shows a significant increase in current ratio (I_{on}/I_{off}) values, reaching a maximum value of 3.5×10^3 with the transistor OTFT-P3HT:GZO_1%, which is the required value to integrate the electronic devices. Additionally, it exhibits a linear increase in saturation field-effect mobility (μ_{sat}), reaching the highest value of 3.2×10^{-3} $cm^{-1}/V.s$ with the transistor OTFT-P3HT:GZO_3%, which represents a 100-fold enhancement. The increase in saturation mobility can be attributed to the improvement in charge carrier transport and reduction in trap density within the active layer of the device due to the generation of free holes resulting from the substitutive incorporation of Ga^{3+} ions into Zn^{2+} cation sites or the incorporation of Ga ions into interstitial positions [18]. These results are extremely interesting for OTFT devices fabricated and characterized both in the dark and ambient conditions. These results hold great promise for the potential use in practical applications, such as low-cost photodetectors and sensor devices.

TABLE 1. Electrical parameters of OTFTs-P3HT:GZO as a function of the Ga doping concentration (from 0 to 3%).

	OTFT-P3HT	OTFT-P3HT:GZO_0%	OTFT-P3HT:GZO_1%	OTFT-P3HT:GZO_2%	OTFT-P3HT:GZO_3%
I_{on}/I_{off}	363	580	3535	1474	112
V_{th} (V)	24	9	6	10	11
SS (V/dec)	4	3.5	3	2.5	3
μ_{sat} (cm^{-1}/V. s)	1.3×10^{-5}	3.4×10^{-5}	3×10^{-4}	5×10^{-4}	3.2×10^{-3}

4. Conclusion

In summary, we have successfully fabricated p-type OTFT devices with bottom gate/bottom-contact configuration based on a hybrid semiconductor layer composed of P3HT polymer enriched by Ga-doped ZnO nanoparticles as an active layer, by using sol-gel coupled with spin-coating method, and they were characterized by various techniques in the dark and under daylight conditions. The investigation of the influence of gallium doping concentration on the OTFT devices based on P3HT:GZO thin-film performance exhibited the capability to regulate both threshold voltage (V_{th}) and hysteresis by adjusting the gallium doping within the active layer. Additionally, the fabricated transistors demonstrated significantly high performance, attaining a current ratio (I_{on}/I_{off}) of 3.5×10^3 with 1% Ga doping and achieving a 100-fold enhancement in field-effect saturation mobility (μ_{sat}) with 3% Ga doping, highlighting their potential for practical applications, including cost-effective photodetectors and sensors.

References

[1] Tang, C.W., Applied Physics Letters, 48 (2) (1986) 183.

[2] Tsumura, A., Koezuka, H., and Ando, T., Applied Physics Letters, 49 (18) (1986) 1210.

[3] Tang, C.W. and VanSlyke, S.A., Applied Physics Letters, 51 (12) (1987) 913.

[4] Kumar, A., Navan, R.R., Kushwaha A., Aslam, M., and Rao, V.R., International Journal of Nanoscience, 10 (2011) 761.

[5] Xie, T., Xie, G., Du, H., Ye, Z., Su, Y., and Chen, Y., Science China Technological Sciences, 59 (2016) 714.

[6] El Ghoul, J., Omri, K., El Mir, L., Barthou, C., and Alaya, S., Journal of Luminescence, 132 (9) (2012) 2288.

[7] Jaballah, S., Benamara, M., Dahman, H., Ly, A., Lahem, D., Debliquy, M., and El Mir, L., Materials Chemistry and Physics, 255 (2020) 123643.

[8] Erouel, M., Mansouri, S., Ba, M., Romero, A., Jiménez-Tejada, J.A., and El Mir, L., Journal of Electronic Materials, 52 (2023) 5315.

[9] El Mir, L., Journal of Luminescence, 186 (2017) 98.

[10] Kim, J. and Yong, K., Journal of Physical Chemistry C, 115 (15) (2011) 7218.

[11] Shrotriya, V., Ouyang, J., Tseng, R.J., Li, G., and Yang, Y., Letters of Physical Chemistry, 411 (1-3) (2005) 138.

[12] Ba, M., Erouel, M., Mansouri, S., Chouiref, L., Jdir, M., and El Mir, L., Sensors and Actuators A: Physical, 359 (2023) 114470.

[13] Nayak, P.K., Yang, J., Kim, J., Chung, S., Jeong, J., Lee, C., and Hong, Y., Journal of Physics D: Applied Physics, 42 (2009) 035102.

[14] Gu, G., Kane, M.G., Doty, J.E., and Firester, A.H., Applied Physics Letters, 87 (2005) 243512.

[15] Paasch, G., Scheinert, S., Herasimovich, A., Hörselmann, I., and Lindner, T., Physica Status Solidi A, 205 (3) (2008) 534.

[16] Bolognesi, A., Berliocchi, M., Manenti, M., Di Carlo, A., Lugli, P., Lmimouni, K., and Dufour, C., IEEE Transactions on Electron Devices, 51 (12) (2004) 1997.

[17] Majewski, L.A. and Grell, M., Synthetic Metals, 151 (2) (2005) 175.

[18] Jun, M.C., Park, S.U., and Koh, J.H., Nanoscale Research Letters, 7 (2012) 1.